

# Joint Optimization on Uplink OFDMA and MU-MIMO for IEEE 802.11ax: Deep Hierarchical Reinforcement Learning Approach

Hyeonho Noh, *Student Member, IEEE*, Harim Lee, and Hyun Jong Yang, *Member, IEEE*

**Abstract**— This letter tackles a joint user scheduling, frequency resource allocation (USRA), multi-input-multi-output mode selection (MIMO MS) between single-user MIMO and multi-user (MU) MIMO, and MU-MIMO user selection problem, integrating uplink orthogonal frequency division multiple access (OFDMA) in IEEE 802.11ax. Specifically, we focus on *unsaturated traffic conditions* where users' data demands fluctuate. In unsaturated traffic conditions, considering packet volumes per user introduces a combinatorial problem, requiring the simultaneous optimization of MU-MIMO user selection and RA along the time-frequency-space axis. Consequently, dealing with the combinatorial nature of this problem, characterized by a large cardinality of unknown variables, poses a challenge that conventional optimization methods find nearly impossible to address. In response, this letter proposes an approach with deep hierarchical reinforcement learning (DHRL) to solve the joint problem. Rather than simply adopting off-the-shelf DHRL, we *tailor* the DHRL to the joint USRA and MS problem, thereby significantly improving the convergence speed and throughput.

**Index Terms**—IEEE 802.11ax, OFDMA, user scheduling, resource allocation, deep hierarchical reinforcement learning.

## I. INTRODUCTION

IEEE 802.11ax, as the inaugural standard capable of concurrently supporting uplink multi-user multi-input multi-output (UL MU-MIMO) and orthogonal frequency division multiple access (OFDMA), has been pivotal since its release [1]. Evidently, tackling the joint user scheduling and resource allocation (USRA) problem that encompasses elements such as UL MU-MIMO, OFDMA, MU-MIMO user selection, and MIMO mode selection (MS) between single-user (SU)-MIMO and MU-MIMO is crucial to optimize the system performance [2], [3]. In particular, the majority of studies [2]–[6] tackling the joint problem have evaluated theoretical spectral efficiency under saturated traffic scenarios, assuming all users possess unlimited packet queues of infinite length. This assumption, however, diverges from real-world conditions, where user traffic is usually unsaturated, i.e., packet volumes can vary across different users, and packet length is subject to stringent constraints. Thus, it becomes imperative to address unsaturated traffic conditions to closely reflect real-world scenarios [7]–[9].

Despite its significance, only a few traffic-aware USRA studies have been researched in the realm of Wi-Fi and 3GPP-based cellular networks. However, these studies avoid inherent explosive complexity by neglecting one or several aspects of the joint problem, as summarized in Table I. Even studies employing deep learning or reinforcement learning (RL), which have been widely employed in addressing complex problems under dynamic natures, have failed to fully account for all

Hyeonho Noh and Hyun Jong Yang are with Department of Electrical Engineering, Pohang University of Science and Technology (POSTECH), Pohang, 37673, Korea (e-mail: {hyeonho, hyunyang}@postech.ac.kr). Harim Lee is with School of Electronic Engineering, Kumoh National Institute of Technology, Gumi, Gyeongbuk, 39248, Korea (e-mail: hrlee@kumoh.ac.kr). Hyun Jong Yang is the corresponding author.

TABLE I

COMPARISON OF THE PROPOSED SCHEME TO PREVIOUS WORKS.

	Ref	US	RA	OFDMA	MIMO MS	Buffer	MU-MIMO	DL/RL
Celluar	[7]	o	x	x	x	o	o	x
	[8]	o	o	o	x	o	o	x
Wi-Fi	[5], [6]	o	o	o	x	x	o	x
	[2]	o	o	o	o	x	o	x
	[3]	o	o	o	o	x	o	o
	[10], [11]	o	o	o	x	o	x	o
	[9]	x	o	o	x	o	x	x
Wi-Fi	Ours	o	o	o	o	o	o	o

aspects of the joint problem. Consequently, these oversights result in notable losses in generality and performance in the existing works. Furthermore, the seamless adaptation of USRA techniques designed for 3GPP-based cellular networks to 802.11ax proves challenging due to the constraints on frequency band utilization in 802.11ax [3], [4].

In this letter, we address the USRA optimization problem which involves UL MU-MIMO, OFDMA, MU-MIMO user selection, and MIMO MS for IEEE 802.11ax uplink under unsaturated traffic conditions. Specifically, we tailor a deep hierarchical RL (DHRL) framework, specialized for solving complex joint problems [12], [13], to the joint problem. After decomposing the USRA problem into a hierarchy of RA and US, we define master and sub-agents for solving RA and US problems, respectively. The proposed DHRL model can adapt to the dynamic wireless environment, enhance the sample efficiency, and improve network performance significantly. Specifically, unlike existing works, we integrate all aspects of the joint problem without any relaxation, ensuring our approach does not incur any loss in generality or performance.

While applying off-the-shelf DHRL directly makes the learning process nearly impractical due to agents' explosive action space size, we refine sub-agents to align with the standard-defined frequency band utilization, markedly improving the practicality and performance of the system. In addition, we propose a state update process based on channels' semiorthogonality, which leads to a huge performance gain.

The rest of this letter is organized as follows: Section II provides a comprehensive overview of the problem formulation. Section III explores the underlying algorithmic framework of the proposed DHRL model. Section IV presents experimental results. The final section concludes the letter.

## II. SYSTEM MODEL AND PROBLEM FORMULATION

### A. Scenario

In the context of IEEE 802.11ax uplink, we consider a basic service set where an access point (AP) communicates with  $K$  stations (STAs). The AP is equipped with  $N_R$  antennas, while each STA employs  $N_T$  antennas. Fig. 1 depicts an illustration of 802.11ax UL data transmission protocol. The AP estimates the uplink channel state information (CSI) through the uplink pilot. Additionally, the AP gathers buffer status reports (BSR) from the STAs by initiating a BSR poll trigger

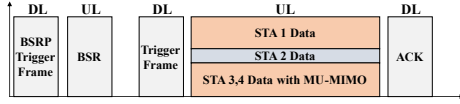


Fig. 1. Illustration of 802.11ax UL data transmission protocol.

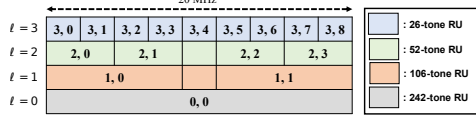


Fig. 2. OFDMA RUs in a 20 MHz channel.

frame and receiving feedback. With the acquired CSI and buffer status information, the AP determines a combination of resource units (RUs), specifically referring to resource blocks in WLAN, for RA. In addition, the AP schedules single or multiple STAs to transmit uplink data on each RU and specifies the number of transmission packets for individual STAs. Subsequently, the AP acknowledges the scheduled STA by transmitting a trigger frame.

### B. OFDMA RU Allocation

According to the IEEE 802.11ax WLAN standard [1], 256 subcarriers are included in a 20 MHz channel. These 256 subcarriers can be grouped into RUs with various sizes, as depicted in Fig. 2. Let  $\text{RU}(l, i)$  denote the RU at the  $l$ -th level and  $i$ -th index. Then, each RU can be allocated to an STA for SU-MIMO or multiple STAs for MU-MIMO uplink data transmission. RUs with 106-tone or larger RUs support both SU-MIMO and MU-MIMO, while RUs with 26- or 52-tone permit only SU-MIMO.

The IEEE 802.11ax WLAN standard [1] prohibits an STA from occupying multiple RUs. Furthermore, the simultaneous allocation of multiple RUs on the same frequency band is forbidden. For example, a valid combination could be  $[\text{RU}(1, 0), \text{RU}(3, 4), \text{RU}(2, 2), \text{RU}(2, 3)]$ . To represent the restrictions, we define  $\mathbf{e}_{l,i,t} \in \mathbb{Z}^{q \times 1}$  as an indicating vector, the  $n$ -th element of which is defined such that  $[\mathbf{e}_{l,i,t}]_n = 1$  if  $\text{RU}(l, i)$  overlaps with  $\text{RU}(L, n)$  in the spectrum domain at the time step  $t$ , and  $[\mathbf{e}_{l,i,t}]_n = 0$  otherwise, where  $q$  is the number of 26-tone RUs,  $[\mathbf{x}]_n$  is the  $n$ -th entry of a vector  $\mathbf{x}$ , and  $L$  is the highest level of RUs (e.g.,  $L = 3$  in the case of a 20 MHz channel). In addition,  $x_{l,i,t}^{(k)}$  is defined as a binary RU assignment variable such that  $x_{l,i,t}^{(k)} = 1$  if the  $k$ -th STA is allocated to  $\text{RU}(l, i)$  at the time step  $t$ , and  $x_{l,i,t}^{(k)} = 0$  otherwise. Then, we can represent the constraints on the RA as follows:

$$\sum_{\forall(l,i)} \delta \left( \sum_{k \in \mathcal{K}} x_{l,i,t}^{(k)} \mathbf{e}_{l,i,t} \right) \preceq \mathbf{1}_p, \quad (1a)$$

$$\sum_{\forall(l,i)} x_{l,i,t}^{(k)} \leq 1, \quad \forall k \in \mathcal{K}, \quad (1b)$$

$$\sum_{k \in \mathcal{K}} x_{l,i,t}^{(k)} \leq G(l), \quad \forall(l, i), \quad (1c)$$

where  $\delta : \mathbb{Z}^{q \times 1} \rightarrow \mathbb{Z}^{q \times 1}$  is the function defined such that  $[\delta(\mathbf{x})]_n = \min\{1, [\mathbf{x}]_n\}$  for a vector  $\mathbf{x}$ ,  $\mathbf{1}_p$  is the  $p$ -dimensional vector defined by  $\mathbf{1}_p = [1, 1, \dots, 1]^T$ ,  $p$  is the number of 26-tone subcarriers,  $G$  is the function such that  $G(l) = 1$  if  $\text{RU}(l, i)$  is either 26- or 52-tone RU, and  $G(l) = \lfloor N_R/N_T \rfloor$  otherwise, and  $\preceq$  is the element-wise inequality operator. Constraint (1a) states that two or more different RUs cannot be allocated on the same frequency band. Constraint (1b) indicates the unique user assignment along all RUs. Constraint (1c) imposes the restriction on MIMO MS, by which MU-MIMO can be employed in RUs with sizes greater than 52-tone.

### C. Throughput Model

Let  $\mathbf{H}_{s,t}^{(k)} \in \mathbb{C}^{N_R \times N_T}$  denote the uplink communication channel between the AP and the  $k$ -th STA on the  $s$ -th subcarrier at the time step  $t$ . After the STAs transmit uplink signals, the AP applies the receive beamformer  $\mathbf{w}_{s,t}^{(k)} \in \mathbb{C}^{N_R \times 1}$  to receive the signal from the  $k$ -th STA on the subcarrier  $s$  at the time step  $t$ . Then, the signal-to-interference-plus-noise ratio (SINR) for the  $k$ -th STA on the subcarrier  $s$  at the time step  $t$  yields

$$\Gamma_{s,t}^{(k)} = \frac{P_{s,t}^{(k)} \left\| \left( \mathbf{w}_{s,t}^{(k)} \right)^H \mathbf{H}_{s,t}^{(k)} \right\|_2^2}{\sum_{m \in \mathcal{K} \setminus \{k\}} P_{s,t}^{(m)} \left\| \left( \mathbf{w}_{s,t}^{(k)} \right)^H \mathbf{H}_{s,t}^{(m)} \right\|_2^2 + \sigma^2},$$

where  $P_{s,t}^{(k)}$  is the transmit power of the  $k$ -th STA on the subcarrier  $s$  at the time step  $t$ ,  $\sigma^2$  is the noise variance, and  $\mathcal{K} = \{0, 1, \dots, K-1\}$ . In this letter, we assume the use of zero-forcing for the receive beamformer. Additionally, we assume  $N_T = 1$  with  $\mathbf{h}_{s,t}^{(k)} \in \mathbb{C}^{N_R \times 1}$  for ease of explanation.

We determine the modulation and coding schemes (MCS) of all the STAs according to the IEEE 802.11ax standard [1]. In particular, we define  $m(\Gamma)$  and  $c(\Gamma)$  as the modulated bits per symbol and the channel coding rate corresponding to the SINR, respectively. Here, it is assumed that channel coherence time is much longer than the OFDM symbol length  $\tau$ . Then, the OFDM rate for the  $k$ -th STA on  $\text{RU}(l, i)$  at the time step  $t$  can be given by  $O_{l,i}^{(k)}(\Gamma_t) = \sum_{s \in \text{RU}(l,i)} m(\Gamma_{s,t}^{(k)}) c(\Gamma_{s,t}^{(k)}) / \tau$ , where  $\Gamma_t$  is the matrix such that  $[\Gamma_t]_{s,k} = \Gamma_{s,t}^{(k)}$ . With the determined OFDM rate, the  $k$ -th STA transmits  $p_t^{(k)}$  packets within the limited physical protocol data unit (PPDU) time  $\tau_{\text{PPDU}}$ . Clearly, the transmission time for  $p_t^{(k)}$  packets can be represented by  $T_{l,i}^{(k)}(\Gamma_t, p_t^{(k)}) = Q p_t^{(k)} / O_{l,i}^{(k)}(\Gamma_t)$ , where  $Q$  is the length of each packet. The data throughput (bits/s) of the  $k$ -th STA on  $\text{RU}(l, i)$  [5] can be represented by

$$R_{l,i}^{(k)}(\mathbf{X}_t, \Gamma_t, \mathbf{p}_t) = \frac{x_{l,i,t}^{(k)} O_{l,i}^{(k)}(\Gamma_t) T_{l,i}^{(k)}(\Gamma_t, p_t)}{\max_{l,i,k} x_{l,i,t}^{(k)} \left( T_{l,i}^{(k)}(\Gamma_t, p_t) + V^{(k)} \right)}, \quad (2)$$

where  $\mathbf{X}_t$  is the three-dimensional data cube such that  $[\mathbf{X}_t]_{l,i,k} = x_{l,i,t}^{(k)}$ ,  $\mathbf{p}_t = [p_t^{(0)}, \dots, p_t^{(K-1)}]$ , and  $V^{(k)}$  is the overhead for the  $k$ -th STA.

### D. Joint USRA Optimization Problem

Considering the constraints on the RA and packet transmission, we formulate the USRA optimization problem as follows:

$$\max_{\mathbf{X}_t, \mathbf{p}_t} \sum_t \sum_k \sum_{\forall(l,i)} R_{l,i}^{(k)}(\mathbf{X}_t, \Gamma_t, \mathbf{p}_t), \quad (3a)$$

$$\text{s.t.} \quad (1a)-(1c), \quad (3b)$$

$$p_t^{(k)} < b_t^{(k)}, \quad \forall k \in \mathcal{K}, \quad (3c)$$

$$\frac{Q p_t^{(k)}}{O_{l,i}^{(k)}(\Gamma_t)} < \tau_{\text{PPDU}}, \quad \forall(l, i), \quad \forall k \in \mathcal{K}, \quad (3d)$$

where  $b_t^{(k)}$  is the buffer status of the  $k$ -th STA at the time step  $t$ . The aim of the problem (3) is to maximize overall data throughput while adhering to the constraint on RA and MIMO MS in (1). Furthermore, the number of transmission packets should be judiciously determined to ensure that STAs do not transmit packets exceeding their buffer status in (3c), and their transmission does not surpass the maximum PPDU time in (3d). Solving the USRA optimization problem (3) proves to be intractable, given its nature as mixed-integer non-linear programming, which has been established as NP-hard. Notably, the USRA optimization problem (3) incorporates aspects such as OFDMA, MU-MIMO, MIMO MS, and buffer status of

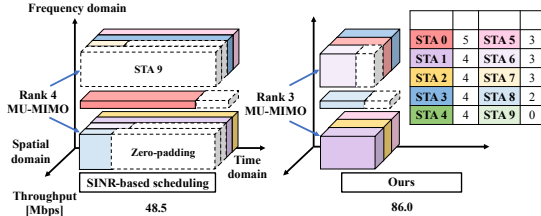


Fig. 3. An illustrative example of the USRA when scheduling STAs and allocating RUs with conventional and proposed methods.

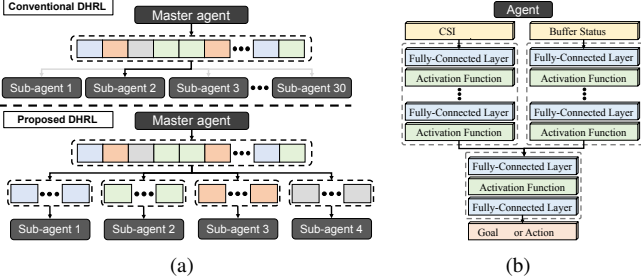


Fig. 4. Illustration of the proposed DHRL model structure. (a) The comparison between the conventional and proposed DHRL model in a 20 MHz channel. A master agent performs RA, and sequentially sub-agents schedule STAs on the allocated RUs. Then, the AP transmits a trigger frame containing the result of USRA to the STAs. (b) The network structure of both master and sub-agents.

the STAs, rendering it more challenging compared to previous works that did not account for all these facets.

### III. PROPOSED DHRL ALGORITHM

#### A. Overview of The Proposed Scheme

Fig. 3 illustrates the importance of considering the buffer status of each STA under unsaturated traffic conditions. The left figure shows inefficiencies of utilizing the semiorthogonal user selection (SUS) algorithm [14] for MU-MIMO user selection and state-of-the-art uplink RA techniques [2] in such conditions. Both algorithms, though near-optimal in saturated traffic conditions by focusing on SINR, lead to inefficiencies when STAs with minimal or empty buffer status but good SINR are scheduled alongside other STAs with large buffer status on the same RU. Hence, long periods of redundant zero padding may be inserted to wait until the end of the other STAs' data transmission. Furthermore, it favorably assigns high-rank MU-MIMO to maximize the sum of SINR. The right figure serves as an example of solving the USRA problem using the proposed DHRL-based method. This method optimizes MU-MIMO user selection and RA along the time-frequency-space axis by factoring in both the STAs' SINRs and buffer status, so that it allows for efficient RA and MU-MIMO designs sometimes with low-rank MU-MIMO, instead of always relying on high-rank MU-MIMO.

#### B. Structure and parameters of the proposed DHRL

Decomposing the USRA problem into a hierarchy of RA and US, an AP defines master and sub-agents on its own, without collaboration with other nodes, each designed for solving RA and US problems, respectively. Here, we define the result of RA as a goal and the result of US as an action. The USRA process begins with the master agent setting a goal  $g_t$ . Unlike conventional DHRL approaches that assign all RUs to a single sub-agent, our model is tailored to the frequency band use cases in 802.11ax. This involves decomposing the RU combination determined by  $g_t$  into individual units based on size, as shown in Fig. 4(a). These segmented RUs are inputs for sub-agents, who select actions  $a_t$  based on the current state and

Goal	RU combinations							
	26	26	26	26	26	26	26	26
0	26	26	26	26	26	26	26	26
1	26	26	26	26	26	26	26	52
2	26	26	26	26	26	52	26	26
3	26	26	26	26	26	52	52	
4	26	26	52	26	26	26	26	26
5	26	26	52	26	26	26		
6	26	26	52	26	52	26	26	
7	26	26	52	26	52		52	
8	52	26	26	26	26	26	26	26
9	52	26	26	26	26	26	52	26
10	52	26	26	26	52	26	26	
11	52	26	26	26	52	52		
12	52	52	26	26	26	26	26	
13	52	52	26	26	26	52		
14	52	52	26	52	26	26	26	
15	52	52	26	52	52	52	52	
16	52	52	-	106				
17	106	-	52	106	52			
18	26	26	26	26	26	106		
19	26	26	52	26	106			
20	52	26	26	26	106			
21	52	52	26	106				
22	106	26	26	26	26	26		
23	106	26	26	26	52			
24	106	26	52	26	26			
25	106	26	52	52				
26	106	-	106					
27	52	52	-	52	52			
28	106	26	106					
29	242							

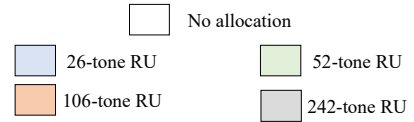


Fig. 5. RU combination table corresponding to goals in a 20 MHz bandwidth channel.

goal. This refined sub-agent structure profoundly optimizes network<sup>1</sup>, enhancing network performance and convergence speed. Finally, the AP constructs  $\mathbf{X}_t$  with the actions and transmits it to the STAs in a trigger frame.

Neural networks typically expect their input data to be homogeneous in terms of format, structure, and characteristics for a given task. However, we hope a single agent to concurrently process both CSI and buffer status, which exhibit heterogeneous characteristics. To this end, we design an agent with two branch neural networks, as shown in Fig. 4(b), each tailored to process either CSI or buffer status, before merging them into the fusion network. This architecture allows for the effective integration of diverse data types, enabling the agent to make more informed decisions based on a comprehensive understanding of the network state.

The state, goal, action, and reward functions of the master agent and sub-agents are defined below.

- *State*: The state for the  $l$ -th level and  $i$ -th index at the time step  $t$  is  $s_t^{(l,i)} = \{\mathbf{H}_{s,t}^{(k)}, b_t^{(k)} | \forall s \in \text{RU}(l,i), \forall k \in \mathcal{K}\}$ . Then, the state for all levels and indices at the time step  $t$  is  $\mathcal{S}_t = \bigcup_{l=0}^L \bigcup_{i \in \mathcal{I}(l)} s_t^{(l,i)}$ , where  $\mathcal{I}(l)$  is the set containing the integer from 0 to the maximum index at the  $l$ -th level.

<sup>1</sup>For example, the sub-agent design reduces the number of sub-agents from 30 to 4 and their action space sizes from  $9.2 \times 10^{10}$  to  $6.2 \times 10^3$  for scenarios with four antennas and 20 STAs in a 20 MHz channel.

- *Goal*: The outcome determined by a master agent regarding the RA is referred to as the goal, and is defined as  $g_t \in \mathcal{G}$ , where  $\mathcal{G}$  is the goal space including all possible cases of RA according to the IEEE 802.11ax standard [1]. A master agent selects a goal, which determines the resource allocation format based on the RU combination table in Fig. 2. For example, if a master agent selects goal 21, the RU combination is [RU(2, 0), RU(2, 1), RU(3, 4), RU(1, 1)]. Subsequently, sub-agents perform user scheduling on each RU. Therefore, sub-agents perform user scheduling on the RU combination corresponding to the selected goal  $g_t$ , [RU( $l_0, i_0$ ), RU( $l_1, i_1$ ), ..., RU( $l_d, i_d$ )].
- *Action*: At the time step  $t$ , we define an action as  $a_t^{(l,i)} \in \mathcal{A}^{(l,i)} = \{S|S \subset \mathcal{K}, |S| \leq G(l)\}$ , where  $\mathcal{A}^{(l,i)}$  is the action space on RU( $l, i$ ). The action  $a_t^{(l,i)}$  specifies the STAs to be scheduled on RU( $l, i$ ) at the time step  $t$ , i.e.,  $x_{l,i,t}^{(k)} = 1$  if  $k \in a_t^{(l,i)}$ . Then, sub-agents supporting MU-MIMO have action spaces of size  $\sum_{i=1}^{\lfloor N_R/N_T \rfloor} \binom{K}{i}$  (constraint (1c)) respectively which are still heavy compared to SU-MIMO. To further reduce the sub-agents' action space sizes, we sophisticatedly redesign the action of sub-agents in section III-C.
- *Reward Function*: After all sub-agents finish the action selection process, a master agent constructs  $\mathbf{X}_t$  with  $a_t^{(l,i)}$  for all levels and indices, executes  $\mathbf{X}_t$ , and obtains extrinsic reward, which is defined by  $\hat{r}_t = \sum_{l=0}^L \sum_{i \in \mathcal{I}(l)} \sum_{k \in \mathcal{K}} R_{l,i}^{(k)}(\mathbf{X}_t, \Gamma_t, \mathbf{p}_t)$ . Given  $\mathbf{X}_t$ ,  $\mathbf{p}_t$  can be constituted using a simple search algorithm with a computational complexity of  $\mathcal{O}(\|\mathbf{X}_t\|_F)$ , where  $\|\mathbf{X}_t\|_F$  represents the number of scheduled STAs. Reward function for sub-agents is defined in section III-C.

### C. Sub-agent design for MU-MIMO

The huge size of previously defined action space stems from the practice of contemplating every possible permutation for MU-MIMO user selection at once. Instead, we propose a sequential user selection approach where  $\lfloor N_R/N_T \rfloor$  decision rounds are sequentially conducted within a single time step, during which sub-agents select one STA per round. To account for scenarios where selecting fewer users than  $\lfloor N_R/N_T \rfloor$  is preferable, sub-agents can choose a 'break' option in any decision round, allowing for the early termination of the selection process. Via the proposed user selection approach, we significantly reduce the action space sizes from  $\sum_{i=1}^{\lfloor N_R/N_T \rfloor} \binom{K}{i}$  to  $K+1$ , which boosts the convergence speed of sub-agent training and improves network performance.

We redefine an action as  $\tilde{a}_t^{(l,i)} \in \mathcal{K} \cup \{break\} = \tilde{\mathcal{A}}$ , where *break* represents the break option, and  $\tilde{\mathcal{A}}$  is the newly defined action space. Across multiple decision rounds, each sub-agent iteratively selects actions. Subsequently, the selected actions are aggregated to form  $a_t^{(l,i)} = \{\tilde{a}_0^{(l,i)}, \dots, \tilde{a}_{T-1}^{(l,i)}\}$ , where  $T$  is the terminal time step. After decision rounds finish, each sub-agent constitutes  $\mathbf{X}_t$  with  $a_t^{(l,i)}$  executes  $\mathbf{X}_t$ , and obtains intrinsic reward,  $r_t^{(l,i)} = \sum_{k \in \mathcal{K}} R_{l,i}^{(k)}(\mathbf{X}_t, \Gamma_t, \mathbf{p}_t)$ .

In contrast to SU-MIMO, MU-MIMO can lead to reduced throughput if there is strong mutual interference among STAs. Therefore, we design a model structure aimed at mitigating mutual interference among selected STAs. To this end, we continuously update and provide the orthogonal components of the STAs' channel with respect to the selected STAs' channels at each decision round, incorporating this information into the sub-agents' states. Thus, we repeatedly calculate  $\mathbf{g}_{s,t,\tilde{t}}^{(k)}$ , the component of the STAs' channels orthogonal to the subspace

### Algorithm 1 Proposed DHQN-based USRA algorithm

- 1: **Initialize:**  $\theta_M, \theta_S^{(l)}, \mathcal{D}_M, \mathcal{D}_S^{(l)}, s_t^{(l,i)}, \forall(l, i)$ .
- 2: **for**  $e = 1, \dots, num\_episodes$  **do**
- 3:   Get start state description  $\mathcal{S}_0, t \leftarrow 0$
- 4:   **while**  $\mathcal{S}_t$  is **not** terminal **do**
- 5:     Select  $g_t$  with a  $\epsilon$ -greedy policy
- 6:     **for**  $j = 0, \dots, d$  **do**
- 7:        $a_t^{(l_j, i_j)} \leftarrow \text{ACTIONSELECTION}(\mathcal{S}_t, (l_j, i_j), e)$
- 8:     **end for**
- 9:     Execute  $a_t$ , and obtain  $\hat{r}_t$  and  $\mathcal{S}_{t+1}$
- 10:     Store  $(\mathcal{S}_t, g_t, \hat{r}_t, \mathcal{S}_{t+1})$  in  $\mathcal{D}_M$
- 11:     Update  $\theta_M$  by the stochastic gradient descent method
- 12:      $t \leftarrow t + 1$
- 13:   **end while**
- 14: **end for**
- 15: **return**  $\mathbf{X}_t$

spanned by  $\{\tilde{\mathbf{g}}_{s,t,1}, \dots, \tilde{\mathbf{g}}_{s,t,\tilde{t}-1}\}$  at each decision round  $\tilde{t}$ , which can be obtained by

$$\mathbf{g}_{s,t,\tilde{t}}^{(k)} = \mathbf{h}_{s,t}^{(k)} - \sum_{j=1}^{\tilde{t}-1} \frac{\left(\mathbf{h}_{s,t}^{(k)}\right)^H \tilde{\mathbf{g}}_{s,t,j}}{\|\tilde{\mathbf{g}}_{s,t,j}\|^2} \tilde{\mathbf{g}}_{s,t,j}, \quad (4)$$

where  $\mathbf{g}_{s,t,1}^{(k)} = \mathbf{h}_{s,t}^{(k)}$  for all  $k \in \mathcal{K}$ ,  $\tilde{\mathbf{g}}_{s,t,j} = \mathbf{g}_{s,t,j}^{(k')}$ , and  $k'$  is the index of selected STA at the  $j$ -th decision round. Then, we utilize  $\mathbf{g}_{s,t,\tilde{t}}^{(k)}$  as new states for MU-MIMO.

### D. DHRL Training Process

We introduce the Deep Q-network (DQN) as the learning framework of the master and sub-agents. Algorithm 1 describes the proposed deep hierarchical Q-network (DHQN)-based USRA. With the newly-defined action  $\tilde{a}$  and action space  $\tilde{\mathcal{A}}$  in section III-C, we train a DHRL model as follows.

1) *Initialization*: We utilize a parameter  $\theta_M$  that defines an action-value function  $Q(\mathcal{S}, g; \theta_M)$  for the master agent and parameters  $\theta_S^{(l)}$  that define action-value functions  $Q(s, a; \theta_S^{(l)}, g)$  for the  $l$ -th level sub-agent, where  $l$  ranges from 0 to  $L$ . In addition, we initialize replay memories  $\mathcal{D}_M$  for the master agent to capacity  $C_M$  and  $\mathcal{D}_S^{(l)}$  for the  $l$ -th sub-agent to capacity  $C_S^{(l)}$ .

2) *Experience collection*: The master agent first selects a goal  $g_t$  with a  $\epsilon$ -greedy policy, where  $\epsilon$  decays from 1.0 to 0.1. For [RU( $l_0, i_0$ ), RU( $l_1, i_1$ ), ..., RU( $l_d, i_d$ )] determined by the selected goal  $g_t$ , each sub-agent selects an action  $a_t^{(l_j, i_j)}$ . Algorithm 2 shows the action selection process in the sub-agents. A sub-agent supporting MU-MIMO repeatedly appends an action  $\tilde{a}_t^{(l_j, i_j)}$  to  $a^{(l_j, i_j)}$  for at most  $\lfloor N_R/N_T \rfloor$  decision rounds. At each decision round  $\tilde{t}$ , the sub-agent evaluates the reward difference  $r_{\tilde{t}}^{(l_j, i_j)} - r_{\tilde{t}-1}^{(l_j, i_j)}$  and stores transition  $(\tilde{s}_{\tilde{t}}^{(l_j, i_j)}, \tilde{a}_{\tilde{t}}^{(l_j, i_j)}, r_{\tilde{t}}^{(l_j, i_j)} - r_{\tilde{t}-1}^{(l_j, i_j)}, \tilde{s}_{\tilde{t}+1}^{(l_j, i_j)})$  in  $\mathcal{D}_S^{(l_j, i_j)}$ . The master agent also stores transition  $(\mathcal{S}_t, g_t, \hat{r}_t, \mathcal{S}_{t+1})$  in  $\mathcal{D}_M$  at each time-step  $t$ .

3) *Updating model parameters*: In each training epoch, we randomly sample mini-batches from the datasets and update the model parameters,  $\theta_M$  and  $\theta_S^{(l)}$ , by the stochastic gradient descent method. In the case of  $\theta_M$ , we set  $y_j = \hat{r}_j$  if  $\mathcal{S}_{j+1}$  is a terminal state or  $y_j = \hat{r}_j + \gamma \max_g Q(\mathcal{S}_{j+1}, g; \theta_M)$ , otherwise. Then, the loss function for a given mini-batch  $\mathcal{B}$  is defined as  $J(\theta_M) = \sum_{j \in \mathcal{B}} (y_j - Q(\mathcal{S}_j, g_j; \theta_M))^2 / |\mathcal{B}|$ . By the stochastic gradient descent method, the parameter  $\theta_M$  is

---

**Algorithm 2** ACTIONSELECTION( $\mathcal{S}_t, (l, i), e$ )
 

---

```

1: if  $l \leq 1$  then  $M \leftarrow \lfloor N_R/N_T \rfloor$  else  $M \leftarrow 1$  end if
2:  $\tilde{s}_0^{(l,i)} \leftarrow s_t^{(l,i)}, r_{-1}^{(l,i)} \leftarrow 0, a^{(l,i)} \leftarrow []$ 
3: for  $\tilde{t} = 0, \dots, M - 1$  do
4:   Select  $\tilde{a}_{\tilde{t}}^{(l,i)}$  with a  $\epsilon$ -greedy policy
5:   if  $\tilde{a}_{\tilde{t}}^{(l,i)} = \text{break}$  then break end if
6:   Append  $\tilde{a}_{\tilde{t}}^{(l,i)}$  to  $a^{(l,i)}$ 
7:   Execute  $a^{(l,i)}$ , obtain  $r_{\tilde{t}}^{(l,i)}$ , and update  $\tilde{s}_{\tilde{t}+1}^{(l,i)}$  from (4)
8:   Store  $(\tilde{s}_{\tilde{t}}^{(l,i)}, \tilde{a}_{\tilde{t}}^{(l,i)}, r_{\tilde{t}}^{(l,i)} - r_{\tilde{t}-1}^{(l,i)}, \tilde{s}_{\tilde{t}+1}^{(l,i)})$  in  $\mathcal{D}_S^{(l)}$ 
9:   Update  $\theta_S^{(l)}$  by the stochastic gradient descent method
10: end for
11: return  $a^{(l,i)}$ 

```

---

updated to minimize the loss function, which yields

$$\theta_M \leftarrow \theta_M - \frac{\alpha_M}{|\mathcal{B}|} \frac{\partial J(\theta_M)}{\partial \theta_M}, \quad (5)$$

where  $\alpha_M$  is the learning rate. In the same way, the sub-agents can update  $\theta_S^{(l)}$ .

### E. Complexity analysis

We find that the integrated part from the branch network for CSI to the fusion network dominates the majority of computational complexity. Thus, we focus on the computational complexity of such a part. Defining the network depth of the integrated part as  $d$ , with the input size of  $K \cdot 2^{L/2}$ , the computational complexity is  $\mathcal{O}(dK^22^L)$ . In addition, the state update process in (4) requires  $\mathcal{O}(MK)$  computation, where  $M$  is the maximum iteration level. Then, the computational complexity of the proposed DHRL algorithm reads  $\mathcal{O}(dMK^32^L)$ . On the other hand, the conventional work [2] requires  $\mathcal{O}(MK^24^L)$ . While our DHRL algorithm requires  $dK$  times more computational effort, it benefits exponentially from wider bandwidths, as reflected by the more favorable exponential term  $2^L$  compared to  $4^L$  in the conventional work.

## IV. SIMULATION RESULTS

We have conducted simulations to evaluate the performance of the proposed DHQN-based USRA algorithm and compare it with baseline methods. A 802.11ax system, where an AP is equipped with  $N_R = 8$  antennas and STAs employ  $N_T = 2$  antennas, is considered with the bandwidth  $B$  set to 20 MHz. For our simulation, we build a MATLAB simulator based on the IEEE standard channel model document [15]. The STAs are dropped randomly within the distance range of 20 m to 100 m. Packet length  $Q$  is 1500 bytes, the maximum PPDU time is 4.848 ms, and packet arrivals follow the Poisson distribution.

For comparison, we consider three baseline USRA methods.

- **SINR-based scheduling:** This method optimizes USRA by adopting the algorithms in [2] and [14], which are proven to be near-optimal solutions under saturated traffic conditions.
- **SINR-based scheduling (fixed RA):** It maximizes the STAs' throughput by optimizing US but with fixed RA. If MU-MIMO and OFDMA are utilized, the algorithm chooses level  $l = \min(L - 2, \lceil \log_2(K \cdot N_R/N_T) \rceil)$  [2].
- **Buffer-based scheduling (fixed RA):** We design a heuristic algorithm that chooses the same combination of RUs in the SINR-based scheduling (fixed RA) algorithm and assigns as many STAs as possible on every RU. The algorithm selects STAs in ascending order of the number of buffers  $b_t^{(k)}$ .

In Fig. 6, we measure the throughput by varying the number of STAs and packet arrival rates. The SINR-based

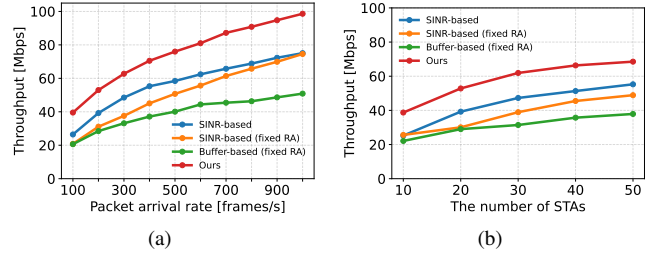


Fig. 6. Throughput of the proposed USRA algorithm and baseline methods with different packet arrival rates and numbers of STAs, respectively. (a) The number of STAs is 20. (b) The packet arrival rate is set to 200 frames/s.

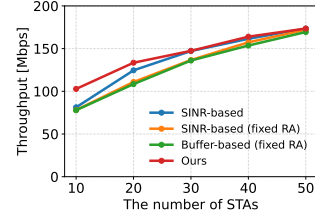


Fig. 7. Throughput of the proposed USRA algorithm and baseline methods with various numbers of STAs. The packet arrival rate is set to 10000 frames/s.

scheduling algorithm shows higher throughput than both SINR and buffer-based methods with fixed RA in addressing the USRA problem, especially under saturated traffic conditions with MU-MIMO and MIMO MS. However, it does not account for the buffer status of STAs. Our method, which includes MU-MIMO, MIMO MS, and STA buffer statuses, outperforms the baselines. At an extreme frame rate of 10000 frames/s, our method achieves throughput levels comparable to or better than the baselines, even in saturated conditions, as shown in Fig. 7. In Fig. 8, we assess the throughput as the number of antennas on the AP and STAs increases. Our method consistently surpasses the baseline in all antenna configurations.

For the ablation study on sub-agent design for MU-MIMO in Sec. III-C, we assess the throughput of the DHQN-based USRA algorithm with and without reduced action space and channel subspace strategy in Fig. 9. The standard DHQN, hindered by vast action spaces, only achieves 70 Mbps. Although the version with reduced action space shows improved throughput, it struggles with generalizing mutual interference among STAs. In contrast, the optimized DHQN effectively addresses the problem of MU-MIMO user selection.

## V. CONCLUSION

This letter proposes a novel DHRL-based USRA algorithm, where a master agent selects a combination of RUs from all possible cases, and sub-agents then schedule STAs to the RUs. We optimize the throughput by contemplating STAs' SINRs and buffer status, so that more efficient utilization of time, frequency, and spatial resources is achieved via the joint design of US, RA, and MU-MIMO. To address the US challenge for MU-MIMO, we propose a sub-agent design with reduced action space and channel subspace strategy. The numerical results show that the proposed algorithm achieves significantly higher throughput than the existing schemes.

## REFERENCES

- [1] "Wireless LAN medium access control (MAC) and physical layer (PHY) specifications," *IEEE Std 802.11ax-2021 (Amendment to IEEE Std 802.11-2020)*, pp. 1–767, 2021.
- [2] K. Wang and K. Psounis, "Scheduling and resource allocation in 802.11ax," in *Proc. IEEE Conf. Comput. Commun. (INFOCOM)*, 2018, pp. 279–287.

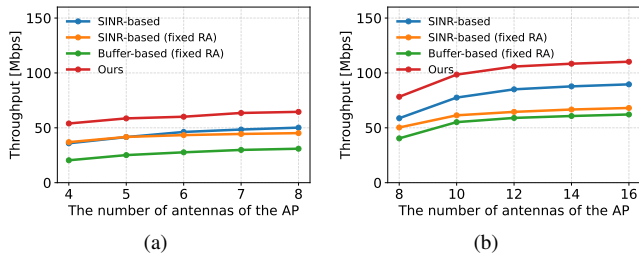


Fig. 8. Throughput across various numbers of antennas for AP and STAs. (a)  $N_T = 1$ . (2)  $N_T = 2$ .

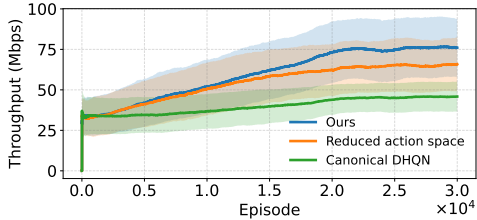


Fig. 9. Throughput of the USRA algorithms with canonical DHQN, reduced action space, and proposed methods. The number of STAs is 20, and the packet arrival rate is set to 500 frames/s.

- [3] P. K. Sangdeh and H. Zeng, "DeepMux: Deep-learning-based channel sounding and resource allocation for IEEE 802.11ax," *IEEE J. Sel. Areas Commun.*, vol. 39, no. 8, pp. 2333–2346, 2021.
- [4] D. Bankov *et al.*, "OFDMA uplink scheduling in IEEE 802.11ax networks," in *Proc. IEEE Int. Conf. Commun. (ICC)*, 2018, pp. 1–6.
- [5] V. N. Ha, G. Kaddoum, and G. Poitou, "Joint radio resource management and link adaptation for multicasting 802.11ax-based WLAN systems," *IEEE Trans. Wireless Commun.*, vol. 20, no. 9, pp. 6122–6138, 2021.
- [6] K.-H. Lee, "Using OFDMA for MU-MIMO user selection in 802.11ax-based Wi-Fi networks," *IEEE Access*, vol. 7, pp. 186 041–186 055, 2019.
- [7] Z. Xie and W. Chen, "A joint channel and queue aware scheduling method for multi-user massive MIMO systems," in *Proc. IEEE Int. Conf. Commun. (ICC)*, 2019, pp. 1–6.
- [8] Y.-H. Liu and K. C.-J. Lin, "Traffic-aware resource allocation for multi-user beamforming," *IEEE Trans. Mob. Comput.*, vol. 22, no. 6, pp. 3677–3690, 2023.
- [9] S. Bhattarai, G. Naik, and J.-M. J. Park, "Uplink resource allocation in IEEE 802.11ax," in *IEEE Int. Conf. Commun. (ICC)*, 2019, pp. 1–6.
- [10] R. Balakrishnan *et al.*, "Deep reinforcement learning based traffic- and channel-aware OFDMA resource allocation," in *IEEE Global Commun. Conf. (GLOBECOM)*, 2019, pp. 1–6.
- [11] D. Kotagiri, K. Nihei, and T. Li, "Distributed convolutional deep reinforcement learning based OFDMA MAC for 802.11ax," in *IEEE Int. Conf. Commun.*, 2021, pp. 1–6.
- [12] T. D. Kulkarni *et al.*, "Hierarchical deep reinforcement learning: Integrating temporal abstraction and intrinsic motivation," in *Proc. Neural Information Processing Systems*, vol. 29, 2016.
- [13] K. Frans, J. Ho, X. Chen, P. Abbeel, and J. Schulman, "Meta learning shared hierarchies," in *Proc. Int. Conf. Learn. Represent. (ICLR)*, 2018.
- [14] T. Yoo and A. Goldsmith, "On the optimality of multiantenna broadcast scheduling using zero-forcing beamforming," *IEEE J. Sel. Areas Commun.*, vol. 24, no. 3, pp. 528–541, 2006.
- [15] *IEEE 802.11ax Channel Model Document*, IEEE 802 Working Groups Std., Sep. 2014.